ACS SyntheticBiology

Research Article

pubs.acs.org/synthbio

Forcefield_NCAA: *Ab Initio* Charge Parameters to Aid in the Discovery and Design of Therapeutic Proteins and Peptides with Unnatural Amino Acids and Their Application to Complement Inhibitors of the Compstatin Family

George A. Khoury, James Smadbeck, Phanourios Tamamis, Andrew C. Vandris, Chris A. Kieslich, and Christodoulos A. Floudas*

Department of Chemical and Biological Engineering, Princeton University, Princeton, New Jersey 08544, United States

Supporting Information

ABSTRACT: We describe the development and testing of *ab initio* derived, AMBER ff03 compatible charge parameters for a large library of 147 noncanonical amino acids including β- and N-methylated amino acids for use in applications such as protein structure prediction and *de novo* protein design. The charge parameter derivation was performed using the RESP fitting approach. Studies were performed assessing the suitability of the derived charge parameters in discriminating the activity/inactivity between 63 analogs of the complement inhibitor Compstatin on the basis of previously published experimental IC_{50} data and a screening procedure involving short simulations and binding free energy calculations. We found that both the approximate binding affinity (K^*) and the binding free energy calculated through MM-GBSA are capable of discriminating between active and inactive Compstatin analogs, with MM-GBSA performing significantly better. Key interactions between the most potent Compstatin analog that contains a noncanonical amino acid are presented and compared to the most potent analog containing only natural amino acids and native Compstatin. We make the derived parameters and an associated web interface that is capable of performing modifications on proteins using Forcefield_NCAA and outputting AMBER-ready topology and parameter files freely available for academic use at http://selene.princeton.edu/FFNCAA. The forcefield allows one to incorporate these customized amino acids into design applications with control over size, van der Waals, and electrostatic interactions.

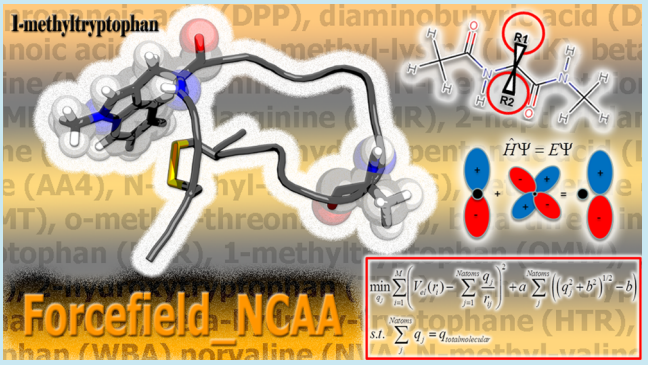

KEYWORDS: *noncanonical amino acids, unnatural amino acids, AMBER partial charges, complement, inhibitors, Compstatin, molecular dynamics*

A timely goal in drug discovery is to have the ability to design new analogs that will stimulate or inhibit a receptor involved in a particular disease process. Several approaches spanning different molecular-weight scales exist to do this. Namely the discovery of small molecules, peptides, peptidomimetics, and high molecular weight antibody therapeutics are all means to create new drugs to address a variety of disease targets. The discovery of such molecules is challenging, with pharmaceutical companies spending billions of dollars each year on the research, development, and optimization of the affinity and bioavailability properties. Problems with pharmacokinetics and bioavailability were estimated to be the cause of 40% of failures in clinical trials,[1] which is troublesome considering the cost of getting a drug to market is approaching $1 billion.[2]

Protein design is increasingly becoming a means to address some of the challenges faced by small molecules. Over 200 peptides, proteins, or antibodies have been marketed as of 2010,[3] and it has been predicted that by 2020 we will see a larger number of peptides as drugs.[4] Protein/peptide design faces its own difficulties though. These include passively permeating the cell membrane, being soluble at biologically relevant concentrations and pH values, and being subjected to proteolytic cleavage, which quickly reduces the half-life. In fact, unmodified peptides cannot circulate in the bloodstream for longer than a few minutes due to proteolytic cleavage,[5] which hinders any potential therapeutic application of the most specific and highest affinity binders that are designed against a target.

Synthetic biology can potentially address several of the limitations of traditional peptide design through the introduction of post-translational modifications (PTMs) and unnatural amino acids. These noncanonical amino acids (NCAAs) are chemical and biological derivatives of the 20 canonical amino acids and upon their introduction can improve both

Received: October 21, 2013
Published: January 6, 2014

Table 1. Examples of Non-canonical Amino Acids Incorporated into Therapeutic Peptide Agonists and Antagonists Targeting Various Diseases

non-canonical amino acid	therapeutic peptide	diseases targeted	source
biphenylalanine 2′-et-4′-ome-biphenylalanine 2-napthylalanine	truncated variant of GLP1-peptide	diabetes	Mapelli et al.[18]
D-amino acids	Rosetta designed peptides	Alzheimer's	Sievers et al.[19]
2-indanylglycine	oxytocin variants	inhibition of uterine motor activity	Bakos et al.[20]
2-napthylalanine	T140 variants	CXCR4/HIV-1	Tamamura et al.[21]
O-methyltyrosine	carbetocin	prevention of uterine atony, induction, and control of postpartum bleeding or hemorrhage	Vlieghe et al.[3]
O-ethyltyrosine	atosiban	delaying the birth in case of premature birth	Vlieghe et al.[3]
1-napthylalanine	angiotensin I variants	hypertension	Kokubu et al.[22]
1-methyltryptophan, 5-methyltryptophan	Compstatin variants	stroke, heart attack, Alzheimer's, asthma, rheumatoid arthritis, systemic lupus	Mallik et al.[23]
cyclohexylalanine			
phosphotyrosine			
aminoisobutyric acid			
N-methylated amino acids			Qu et al.[24]

pharmacokinetic and pharmacodynamic properties of a peptide−drug candidate while maintaining some of the core of the side-chain scaffold to preserve key interactions. Additionally, backbone N-methylated and D-amino acids are a viable approach to block proteolytic cleavage and improve metabolic stability.[6] From a protein design standpoint, they offer the ability to diversify the sequence space remarkably. A 10 amino acid peptide has a sequence space of $20^{10} = 1.024 \times 10^{13}$. Considering the 20 amino acids and the over 400 PTMs that exist[7,8] in nature, the sequence space of that same 10-amino acid peptide becomes $420^{10} = 1.71 \times 10^{26}$, and that only accounts for the L-amino acids. Thus, introduction of modified amino acids as design choices substantially expands the complexity of reaching the globally optimal design solution as was pointed out in a recent review.[9]

It is not well understood how NCAAs affect protein structure. Unnatural amino acids have been shown to have utility in rational design applications, and thus, binding data exists of peptide analogues containing unnatural amino acids and corresponding performance metrics including K_D and IC_{50}/EC50s. Modified amino acids can change the local electrostatic and conformational environment of a protein and may cause a variety of downstream biological responses.[10] Although incorporation of NCAAs has been shown to change the affinity and inhibitory/stimulatory potency of a peptide, it is currently difficult to pursue rationalizations into the key interactions contributing to that increase due to lack of forcefields to model them.

Experimentally, one can incorporate noncanonical amino acids by peptide synthesis,[11] through bio-orthogonal chemistry,[12,13] or genetically.[14−16] Evolution so far has been unable to address NCAA design naturally, as the machinery to incorporate NCAAs does not exist in most organisms. Even though most organisms have not evolved to incorporate NCAAs, this does not imply that they are not beneficial; it means that there are reasons for why they were not incorporated. These reasons include the toxicity of some of the building blocks and precursors to the noncanonical amino acid, the lack of a metabolic pathway in an organism to create the building block, the inability of the NCAA to be incorporated to permeate the cytoplasm,[16] the lack of a modified aminoacyl tRNA synthetase that can accept the modified amino acid, the lack of an expanded genetic code in the organism, or the lack of a tRNA to decode a modified genetic code. There have been examples where each of these reasons has been successfully engineered.[16,17] Despite organisms having limited ability to naturally incorporate NCAAs, we have derived means to synthetically introduce them.

Complicating the matter is that it is prohibitively expensive to screen a large library of noncanonical amino acid designs. Even the cost of incorporating a few modified amino acids is often an order of magnitude higher than the same scaffold sequence with only natural amino acids. The extreme cost is attributed to raw materials, synthesis, and purification costs, which contribute their own unique difficulties and require attention. These difficulties can be overcome with attention to each modification's characteristics but do not make the screening of large libraries of modified amino acids on peptides or proteins tractable. Nonetheless, there exist many examples where noncanonical amino acids were experimentally incorporated into therapeutic peptides targeting different disease and functional processes, as shown in Table 1. A novel approach that can computationally screen potential analogues and has agreement with experimental data would offer a competitive advantage to its possessor.

Several groups have created methods to design proteins and peptides containing natural amino acids computationally that have been experimentally validated. RosettaDesign[25] has been applied to design a number of different peptides to bind to targets,[26−28] as well as design enzymes for diverse applications.[29−33] Citizen-scientists have applied algorithms available in the Rosetta suite of tools to design a new enzyme for higher Diels-Alderase activity using an online multiplayer game.[34] An iterative optimization approach has been created and applied to designing chimeric variants of dihidrofolate reductase[35] and to switch the cofactor preference of an enzyme.[36] Until recently, methods for computational design only addressed the natural amino acids. Kuhlman and co-workers[37] have recently extended the Rosetta[25] suite of tools to be able to handle several noncanonical amino acids, constructed an extended rotamer library, and used the parameters with Rosetta to perform design to derivatize peptides based on calpastatin to calpain-1. Zagrovic and co-workers have created parameters[38] and tools[39] for a library of modified amino acids compatible with the GROMACS simulation engine.

The Floudas group had notable success designing peptides with natural amino acids that have been validated experimentally on 6 protein targets, producing inhibitors and agonists of proteins that are linked to different diseases.[40−49,53] These designs include entry inhibitors of HIV gp41,[42] agonists

Table 2. Table of Modified Amino Acids for Which Charge Parameters Are Presented in This Work Grouped by Scaffold Amino Acid[a]

alanine	phenylalanine	asparagine	aspartic acid	cysteine
α-aminoisobutyric acid (AIB)	(R)-α-methyl-phenylalanine (MPH)	N4-methyl-asparagine (MEN)	N-methylaspartic acid (NMD)	(R)-L-α-methylcysteine (MCY)
2-aminobutyric acid (ABA)	2-ethyl-4-O-methyl-biphenylalanine (TEF)	(2s,4s)-2,5-diamino-4-hydroxy-5-oxopentanoic acid (GHG)	2-amino-propanedioic acid (FGL)	cysteine acetamide (YCM)
adamanthane (ADA)	3-methyl-biphenylalanine (TMB)	glutamine hydroxamate (HGA)	3-methyl-aspartic acid (2AS)	N-methylcysteine (NMC)
2-aminoheptanoic acid (AHP)	3-O-methyl-biphenylalanine (TOM)	N-methyl-asparagine (NMN)	2-amino-6-oxopimelic acid (26P)	carboxymethylated cysteine (CCS)
3-cyclopentylalanine (CP3)	2-ethyl-biphenylalanine (EBP)	β-asparagine (NBA)	β-aspartic acid (DBA)	benzylcysteine (BCS)
diethylalanine (DLE)	2-methyl-4-O-methyl-biphenylalanine (MFO)	**tryptophan**	**glycine**	s-(2-hydroxyethyl)-cysteine (OCY)
R(+)-α-Allylalanine (AAL)	2-methyl-biphenylalanine (MBP)	5-methyltryptophan (MTR)	2-indanyl-glycine (IGL)	s-acetonylcysteine (CSA)
(R)-α-ethyl alanine (REA)	biphenylalanine (BFA)	1-methyltryptophan (OMW)	vinylglycine (LVG)	β-cysteine (CBA)
(S)-α-ethyl alanine (SEA)	2-methylphenylalanine (MH2)	N-methyltryptophan (NMW)	phenylglycine (004)	**methionine**
cyclohexylalanine (ALC)	3-methylphenylalanine (APD)	2-hydroxytryptophan (TRO)	4-hydroxyphenylglycine (D4P)	hydroxyl-methionine (ME0)
1-napthylalanine (ALN)	4-methylphenylalanine (4PH)	4-amino-tryptophan (4IN)	(2s)-amino(3,5-dihydroxyphenyl)-ethanoic acid (3FG)	ethionine (ESC)
2-napthylalanine (NAL)	4-tert-butyl-phenylalanine (TP4)	6-methyltryptophan (TR6)	N-methylglycine (NMG)	N-methyl-methionine (MME)
5-hydroxy-1-napthalene (NO1)	4-amino-phenylalanine (HOX)	5-methoxytryptophan (MT5)	2-allyl-glycine (2AG)	β-methionine (MBA)
6-hydroxy-2-naphthalene (NO2)	4-methoxy-phenylalanine (0A1)	β-hydroxy-tryptophane (HTR)	β-glycine (GBA)	**leucine**
3-(9-anthryl)-alanine (ANT)	*m*-amidinophenyl-3-alanine (APM)	5-hydroxytryptophan (HRP)	**valine**	*t*-butyl-leucine (BUG)
3-(2-pyridyl)-alanine (PY2)	4-carbamimidoyl-phenyl-alanine (0BN)	β-tryptophan (WBA)	(R)-(+)-α-methylvaline (MVL)	norleucine (NLE)
3-(3-pyridyl)-alanine (PY3)	4-hydroxymethyl-phenyl-alanine (4HP)	**tyrosine**	norvaline (NVA)	5-oxo-norleucine (ONL)
3-(4-pyridyl)-alanine (PY4)	3-ethyl-phenylalanine (DMP)	O-methyltyrosine (OMY)	N-methyl-valine (MVA)	N-methyl-leucine (MLE)
3-(2-quinolyl)-alanine (Q32)	3,4-dimethylphenylalanine (D34)	O-ethyltyrosine (OEY)	β-valine (VBA)	homoleucine (HLE)
3-(3-quinolyl)-alanine (Q33)	phenylserine (BB8)	O-allyltyrosine (OAY)	**threonine**	(R)-α-methylleucine (RML)
3-(4-quinolyl)-alanine (Q34)	homophenylalanine (HPE)	N-methyltyrosine (NMY)	N-methylthreonine (NMT)	β-hydroxyleucine (HLU)
3-(5-quinolyl)-alanine (Q35)	3,3-diphenylalanine (DIF)	O-tyrosine (OTY)	*o*-methyl-threonine (OLT)	hydroxynorvaline (VAH)
3-(6-quinolyl)-alanine (Q36)	kynurenine (KYN)	3-amino-tyrosine (TY2)	β-threonine (TBA)	β-leucine (LBA)
3-(8-hydroxyquinolin-3-yl)-alanine (HQA)	N-methyl-phenylalanine (MEA)	3-amino-6-hydroxy-tyrosine (TYQ)	**lysine**	**serine**
N-methylalanine (NMA)	β-phenylalanine (FBA)	(β-R)-β-hydroxy-tyrosine (OMX)	(R)-α-methylornithine (RMO)	homoserine (HSE)
1-pyrenylalanine (PAL)	**isoleucine**	β-tyrosine (YBA)	(S)-α-methylornithine (SMO)	2-amino-5-hydroxypentanoic acid (LDO)
(R)-2-(2′-propenyl)-alanine (PRP)	N-methylisoleucine (NMI)	**glutamic acid**	2,3-diaminopropanoic acid (DPP)	6-hydroxy-norleucine (AA4)
(R)-2-(4′-pentenyl)-alanine (PEN)	allo-isoleucine (IIL)	N-methylglutamic acid (NME)	diaminobutyric acid (DAB)	N-methyl-serine (NMS)
(R)-2-(7′-octenyl)-alanine (OCT)	3-methyl-alloisoleucine (I2M)	(3r)-3-methyl-glutamic acid (LME)	(2s)-2,8-diaminooctanoic acid (HHK)	β-serine (SBA)
β-alanine (AAB)	β-isoleucine (IBA)	(3s)-3-methyl-glutamic acid (MEG)	N-methyl-lysine (NMK)	**histidine**
glutamine	**arginine**	2s,4r-4-methylglutamate (SYM)	β-lysine (KBA)	N-methylhistidine (NMH)
N-methylglutamine (NMQ)	N-methylarginine (NMR)	5-*o*-methyl-glutamic acid (GME)		
N5-methyl-glutamine (MEQ)				
3-methyl glutamine (LMQ)				
β-glutamine (QBA)				

[a]Corresponding three-letter codes are listed in parentheses following each amino acid.

dx.doi.org/10.1021/sb400168u | ACS Synth. Biol. 2014, 3, 855−869

Table 3. Data Set Used for Testing the Optimized Charges Introduced in Forcefield_NCAA[a]

analog	source	sequence	SeqID	IC_{50} (μM)
1	pharmacophore	Ac-ICV(PTR)QDWGAHRCI-NH2	28	9.60
2	pharmacophore	Ac-RCVVQDWGHHRCT-NH2	17	8.00
3	pharmacophore	Ac-LCVVQDWGWHRCG-NH2	15	5.40
4	pharmacophore	Ac-ICVWQDWGWHRCT-NH2	24	3.10
5	pharmacophore	Ac-ICVVNDWGHHRCT-NH2	3	4.20
6	structurekinetic	Ac-ICV(OMY)QDWGAHRCT-NH2	5	1.30
7	pharmacophore	Ac-MCVHQDWGGHRCF-NH2	16	85.20
8	pharmacophore	Ac-ICVWQDWGHHRCT-NH2	2	2.20
9	structurekinetic	Ac-ICV(MTR)QDWGAHRCT-NH2	3	0.87
10	novel analogues	Ac-ICVYQDWGAHRC(NMT)-NH2	12	1.90
11	pharmacophore	Ac-ICV(OMW)QDWGAHRCT-NH2	1	0.21
12	pharmacophore	Ac-ICVSQDWGHHRCT-NH2	20	50.90
13	pharmacophore	Ac-ICVVQDWGHHSCT-NH2	10	25.00
14	pharmacophore	Ac-ICVVQDWGHHRCI-NH2	13	3.20
15	structurekinetic	Ac-ICVWQDWG(AIB)HRCT-NH2	12	1.50
16	pharmacophore	Ac-ICVWQDWGAHRCT	25	2.00
17	pharmacophore	Ac-ICVVNDWGHHACT-NH2	11	60.00
18	novel analogues	Ac-ICVYQDWGAHR(NMC)T-NH2	11	154.00
19	structurekinetic	Ac-ICV(PAL)QDWGAHRCT-NH2	9	1.20
20	pharmacophore	Ac-ICV(ALC)QDWGAHRCT	27	53.60
21	pharmacophore	Ac-ICVHQDWGHHRCT-NH2	21	10.50
22	pharmacophore	Ac-ICVVQDWGAHACT-NH2	12	9.90
23	structurekinetic	Ac-ICVWQDWGAHRCT-NH2	0	1.20
24	pharmacophore	Ac-ICVWQD(OMW)GAHRCT-NH2	4	1000.00
25	pharmacophore	Ac-ICLVQDWGHHRCT-NH2	8	10.00
26	pharmacophore	Ac-ICVYQDWGAHRCT-NH2	23	3.80
27	structurekinetic	Ac-ICVYQDWGAHRCT-NH2	4	2.40
28	pharmacophore	Ac-ICVWQDWG(AIB)HRCT-NH2	29	1.50
29	structurekinetic	Ac-ICVVQDWGHHRCT-NH2	15	4.50
30	pharmacophore	Ac-ICVAQDWGAHRCI-NH2	7	12.00
31	pharmacophore	Ac-ICLVNDWGHHRCT-NH2	9	8.30
32	novel analogues	Ac-ICVYQD(NMW)GAHRCT-NH2	6	25.00
33	pharmacophore	Ac-ICV(ALN)QDWGAHRCT	31	1.80
34	pharmacophore	Ac-ICVTQDWGHHRCT-NH2	19	68.30
35	novel analogues	Ac-ICVYQ(NMD)WGAHRCT-NH2	5	44.00
36	novel analogues	Ac-ICVYQDW(NMG)AHRCT-NH2	7	584.47
37	novel analogues	Ac-ICVY(NMQ)DWGAHRCT-NH2	4	33.00
38	novel analogues	Ac-ICVYQDWGAHRCT-NH2	0	2.40
39	pharmacophore	Ac-LCVWQDWGRHQCF-NH2	14	131.00
40	pharmacophore	Ac-ICVFQDWGHHRCT-NH2	22	10.20
41	novel analogues	Ac-ICVYQDWGAH(NMR)CT-NH2	10	32.00
42	novel analogues	Ac-ICVYQDWGA(NMH)RCT-NH2	9	94.00
43	structurekinetic	Ac-ICV(OMW)QDWGPHRCT-NH2	14	0.54
44	pharmacophore	Ac-DCVVQDWGHHRCT-NH2	18	22.00
45	structurekinetic	Ac-ICV(OEY)QDWGAHRCT-NH2	6	1.30
46	novel analogues	Ac-ICVYQDWG(NMA)HRCT-NH2	8	1000.00
47	pharmacophore	CVVQDWGHHRC-NH2	del1	33.00
48	pharmacophore	CVVQDWGHC-NH2	del9	600.00
49	novel analogues	Ac−I(NMC)VYQDWGAHRCT-NH2	1	7.50
50	novel analogues	Ac-ICV(NMY)QDWGAHRCT-NH2	3	1000.00
51	pharmacophore	Ac-ICVVGDWGHHRCT-NH2	6	567.00
52	pharmacophore	CVVQDWGHHRCT-NH2	del0	25.00
53	pharmacophore	ICVVQDWGHHRCT	0	12.00
54	pharmacophore	IAVVQDWGHHRAT	5 (Linear)	600.00
55	pharmacophore	CVVQDWC-NH2	del8	600.00
56	pharmacophore	CAVQDWGHHRC	del10	1200.00
57	pharmacophore	CWGHHRCT-NH2	del4	600.00
58	pharmacophore	CVVQDWAHHRC	del11	1200.00
59	pharmacophore	CVQDWGHHRCT-NH2	del7	600.00
60	pharmacophore	CQDWGHHRCT-NH2	del6	600.00
61	pharmacophore	CDWGHHRCT-NH2	del5	600.00

dx.doi.org/10.1021/sb400168u | ACS Synth. Biol. 2014, 3, 855−869

Table 3. continued

analog	source	sequence	SeqID	IC_{50} (μM)
62	pharmacophore	CHHRCT-NH2	del2	600.00
63	pharmacophore	CGHHRCT-NH2	del3	600.00

[a]The noncanonical amino acids studied are phosphotyrosine (PTR), O-methyltyrosine (OMY), N-methylthreonine (NMT), 5-methyltryptophan (MTR), 1-methyltryptophan (OMW), α-aminoisobutyric acid (AIB), N-methylcysteine (NMC), 1-pyrenylalanine (PAL), cyclohexylalanine (ALC), N-methyltryptophan (NMW), 1-naphthylalanine (ALN), N-methylaspartic acid (NMD), N-methylglycine (NMG), N-methylglutamine (NMQ), N-methyl-arginine (NMR), N-methylhistidine (NMH), O-ethyltyrosine (OMY), N-methylalanine (NMA), N-methyltyrosine (NMY). Several of these non-canonical amino acids were substituted in different positions on the Compstatin sequence. ACE and NH2 correspond to the N-terminal and C-terminal blocking groups acetyl and amide to keep the termini neutrally charged.

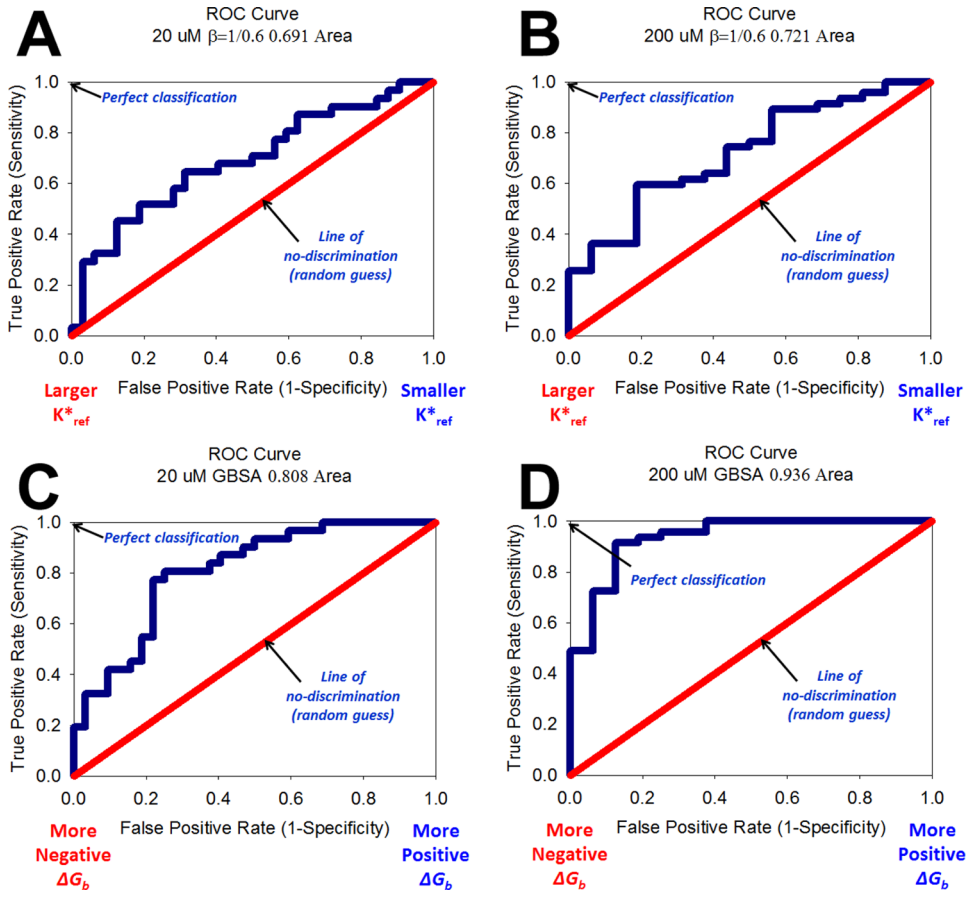

Figure 1. Receiver operating characteristic (ROC) curves constructed from rank-ordered lists of Compstatin variants' binding metrics. ROC curve for rank ordered list by K^* corresponding to an active IC_{50} cutoff of <20 μM (A) and 200 μM (B). ROC curve for rank ordered list by $\Delta G^{\circ GBSA}_{Bind,Solv}$ to an active IC_{50} cutoff of <20 M (C) and 200 μM (D).

and antagonists of the Complement component C3a receptor,[45] inhibitors of Complement component C3c,[40,41,43,47,49,53] and the redesign of human β-defensin-2.[44] We recently developed Forcefield_PTM,[50] a set of AMBER parameters for 32 frequently occurring post-translational modifications. Here, we present new forcefield charge parameters and a web interface to allow for the introduction of 147 noncanonical amino acids into peptides and proteins. The optimized charge parameters are validated on their ability to discriminate between active and inactive analogs of Compstatin for the inhibition of complement component C3c with approximate binding affinity and binding free energy calculations. Subsequently, the new forcefield parameters are used to understand the precise interactions in the most potent Compstatin analog containing a noncanonical amino acid compared with its unmodified counterpart and the original native sequence. Thus, with this new parameter set, we can understand how unnatural amino acids affect binding and other structural properties through molecular simulations.

RESULTS AND DISCUSSION

New Forcefield Charge Parameters for 147 Non-Canonical Amino Acids. Partial charges were calculated for every atom in the library of 147 noncanonical amino acids listed in Table 2 in accordance with the ff03 methodology.[51] The new parameters for each NCAA are presented in the Supporting Information section "Forcefield Parameters for Each Non-canonical Amino Acid Modification Grouped by Scaffold Residue" and are freely available for download and direct import into AMBER at http://selene.princeton.edu/FFNCAA. Conventions for atom and three-letter code naming were done mainly in line with corresponding CIF files contained in the PDB when contained there so the parameters can be used directly with corresponding input PDB files. Images of each

dx.doi.org/10.1021/sb400168u | ACS Synth. Biol. 2014, 3, 855−869

NCAA are also provided in the Supporting Information with all atoms explicitly labeled.

With the determination of these parameters, we next present the results of our efforts to test the parameters on experimental binding data and subsequently to understand the key interactions involved in the most potent Compstatin analog in Table 3 containing the unnatural amino acid 1-methyltryptophan relative to its scaffold sequence.

Predictive Ability of Approximate Binding Affinity in Discriminating Active and Inactive Analogs of Compstatin. Independent molecular dynamics simulations for all 63 Compstatin variants reported in Table 3 were carried out in complex with C3c and in isolation. An independent simulation of the protein C3c without the peptide bound was also carried out. The approximate binding affinity was calculated as in eq 7 (see Methods). The analogs were rank ordered by K^* from highest to lowest. Then, an ROC curve was constructed to assess the predictive ability of the approximate binding affinity metric to discriminate between active and inactive analogs. Two cutoffs were chosen for defining whether an analog was active or inactive: 20 μM and 200 μM.

Parts A and B of Figure 1 present the results of the predictive ability of this metric for this system using the forcefield parameters derived. The approximate binding affinity metric can reasonably discriminate between active and inactive analogs with areas under the ROC curve of 0.691 and 0.721 corresponding to a cutoff for active analogs with IC_{50} < 20 μM and <200 μM, respectively. Only 1 false positive was observed in the top 10 ranked analogs by K^*, and 6 false positives by the 20 μM IC_{50} cutoff were observed in the top 20. This result is encouraging, since K^* has previously been used as the final discriminating metric in our *de novo* protein design framework[42,43,46] using only natural amino acids. This suggests that K^* can be used to reasonably discriminate between active/inactive analogs for new designs of Compstatin with the AMBER energy function and molecular dynamics simulations.

Predictive Ability of Binding Free Energy Calculations in Discriminating Active and Inactive Analogs of Compstatin. An independent molecular dynamics simulation of the complex with each of the 63 variants of Compstatin and C3c was carried out. Snapshots from the simulations were used to perform MM-GBSA calculations to evaluate the binding free energies of each analog. Parts C and D of Figure 1 present the results of the ability for MM-GBSA to discriminate between active and inactive analogs. Binding free energy calculations performed using the forcefield parameters and MM-GBSA yielded the greatest discriminatory ability with areas under the ROC curve of 0.808 and 0.936 corresponding to a cutoff for active analogs with IC_{50} < 20 μM and <200 μM, respectively. This suggests that using the forcefield parameters with MM-GBSA can accurately discriminate between active and inactive analogs of Compstatin. In fact, in the top 10 sequences' calculated $\Delta G^{oGBSA}_{Bind,Solv}$, there was only 1 false positive for either of the IC_{50} cutoffs (in the seventh position), and 6 false positives in the top 20 sequences. Removing the sequences corresponding to deletions of Compstatin in order to compare only equal sequence-length analogs yields an area under the curve of 0.702 and 0.869 for a cutoff IC_{50} of <20 μM and <200 μM, respectively.

We next asked whether there exists a correlation observed between experimental IC_{50} and calculated binding free energy as IC_{50} values were found to be strongly correlated (R^2 = 0.887) with K_D values in the work of Magotti and co-workers.[52] IC_{50} data was used over K_D due to the much larger number of experimental data points available for this system, important for achieving statistical significance in the results. Ideally, a larger number of K_D values would be available to perform similar assessments. We observed a weak correlation between IC_{50} and binding free energy in Figure 2. The existence of a correlation is in agreement with data presented by Magotti.[52]

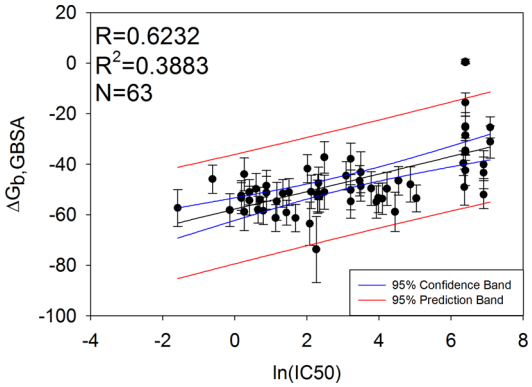

Figure 2. Correlation between IC_{50} and calculated binding free energies using MM-GBSA for 63 Compstatin analogs. The blue bands correspond to the 95% confidence interval for the regression line. The red bands correspond to the 95% confidence interval for a new value to lie in the prediction band. Error bars are ±1 standard deviation from the mean binding free energy calculated.

It is interesting that the binding free energy metric performed better than the approximate binding affinity (K^*), since the approximate binding affinity of each analog compared to the template sequence has been used as the final discriminator of which analogs to send for experimental testing in our *de novo* design framework,[46] and has been successfully applied to designing inhibitors of HIV entry[42] and inhibitors of Complement activation[43] previously. This suggests that we should use the calculated binding free energy if possible instead of the approximate binding affinity when designing new Compstatin variants. Despite these results, the approximate binding affinity calculation will still be useful to assess the docking of complexes when the binding mode is unknown. Additional testing with different sets of protein/peptide complexes beyond C3c/Compstatin should be evaluated in the future to provide further evidence supporting the use of these binding evaluation metrics. Similarly, future testing with different systems having more experimental K_D data can be performed.

Discriminating Differences in Interactions in Compstatin Analogs with Natural and Modified Amino Acids. Due to the new forcefield parameters derived in this work, we have the capability to discriminate interfacial interactions involving noncanonical amino acids at atomistic detail. The most potent analog of Compstatin in Table 3 contains the noncanonical amino acid 1-methyltryptophan in position 4. We aimed to gain insight as to why this substitution is more potent than the analog W4A9 and native Compstatin based on strengths of residue−residue interactions. Therefore, for multiple independent simulation trajectories of analogs W4(OMW)A9, W4A9, and native Compstatin (Sequence 11: Ac-ICV(OMW)QDWGAHRCT-NH2, Sequence 23: Ac-ICVWQDWGAHRCT-NH2, and Sequence 53: ICVVQDWGHHRCT in Table 3), we decomposed the polar and nonpolar interaction free energy contributions and present

dx.doi.org/10.1021/sb400168u | ACS Synth. Biol. 2014, 3, 855−869

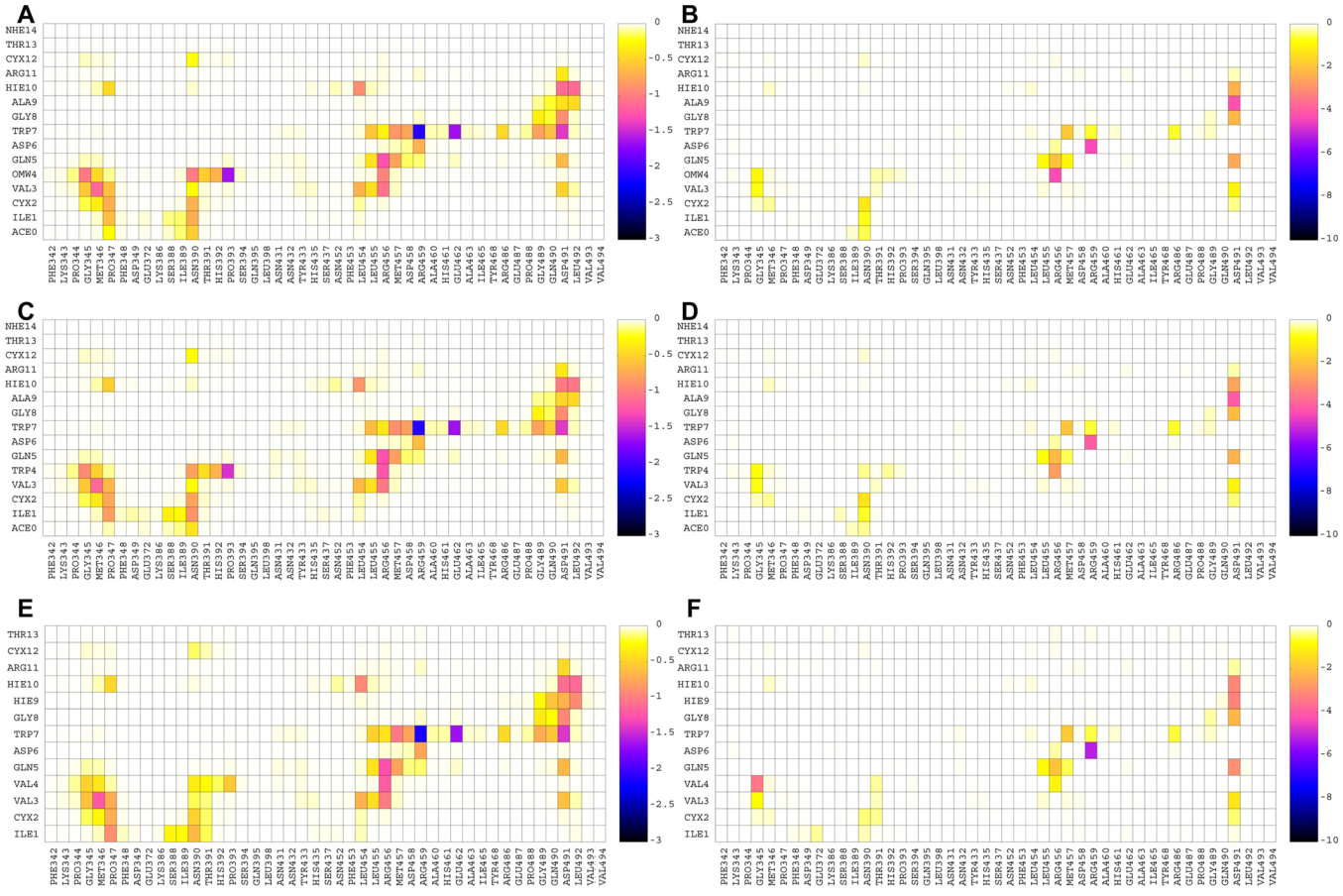

Figure 3. (A) Nonpolar and (B) polar interaction maps for analog W4(OMW)A9. (C) Nonpolar and (D) polar interaction maps for analog W4A9. (E) Nonpolar and (F) polar interaction maps for native Compstatin. The color bar represents the interaction free energy between the corresponding residue−residue pairs in kcal/mol. The color bar was scaled to be the same for the nonpolar and polar interaction free energy contributions so that the different analogues' energetic contributions can be directly compared.

the results of the average interaction free energies as two-dimensional density maps in Figure 3. Here, we focus on differences in interactions due to 1-methyltryptophan relative to tryptophan or valine present in other Compstatin sequences. A full detailed analysis of all pairwise interactions is presented in Supporting Information section "Use of FF_NCAA to Discriminate Specific Contributing Interactions to Antagonistic Activity for Unnaturally Modified Analog Compared to Native and Variant E1 Compstatin."

The substitutions of Val4 to Trp4 and from Trp4 to W4(OMW) result in an increase of the overall nonpolar interactions between residue 4 and C3c residues Gly345, Met346, Asn390, Thr391, His392, Pro393, and Arg456; the increase is more pronounced in the 390−393 C3c residue moiety, as was previously proposed through molecular modeling by Magotti and co-workers.[52] During the simulations of analog W4(OMW)A9, the methyl group of Trp4 is frequently found to lay upon the Cys2-Cys12 disulfide bridge, and this leads to increased intramolecular nonpolar interactions between Trp4 and Cys2-Cys12. Similar behavior was observed in recently published MD computational studies[53] investigating two novel analogs, R1W4(OMW)A9 and R-1S0W4(OMW)A9, which also contain 1-methyltryptophan in position 4 and using the CHARMM forcefield.[54] W4(OMW) forms increased intra- and intermolecular interactions compared with the less potent analogs containing Trp4 and Val4. In all systems, the backbone N in Val/Trp4 is hydrogen bonded to C3c Gly345 O, and the backbone O in Val/Trp4 is hydrogen bonded to the charged amide group of C3c Arg456; the former hydrogen bond-related polar interaction is stronger in the parent Compstatin, whereas the latter is stronger in W4(OMW)A9. The full set of intermolecular interactions formed between the Compstatin analogs and C3c residues in Figure 3 are in agreement with the X-ray structure of W4A9 in complex with C3c[55] and with all previous MD simulation studies in explicit water solvent[49,56,57] using the CHARMM forcefield. Despite the specific differences between the analogs, overall, the strengths of the residue pairwise interaction free energies of the three systems were similar.

FF_NCAA Web Interface. To disseminate the ability to use FF_NCAA to the broader academic community, we have also created a web interface http://selene.princeton.edu/FFNCAA, as shown in Figure 4. The interface allows one to upload a PDB structure to be modified by single or multiple noncanonical amino acids and/or simultaneously mutated. Additionally, the interface allows a user to download the forcefield parameters calculated and derived for FF_NCAA, as well as read instructions for use with AMBER directly.

After user submission, the interface performs the requested modifications and minimizes the structure to remove any clashes that have been formed by introducing the noncanonical amino acid to the nearest local minimum. This step utilizes the parameters from FF_NCAA for the noncanonical amino acids coupled with the parameters in ff03.[51] After completion, the

dx.doi.org/10.1021/sb400168u | ACS Synth. Biol. 2014, 3, 855−869

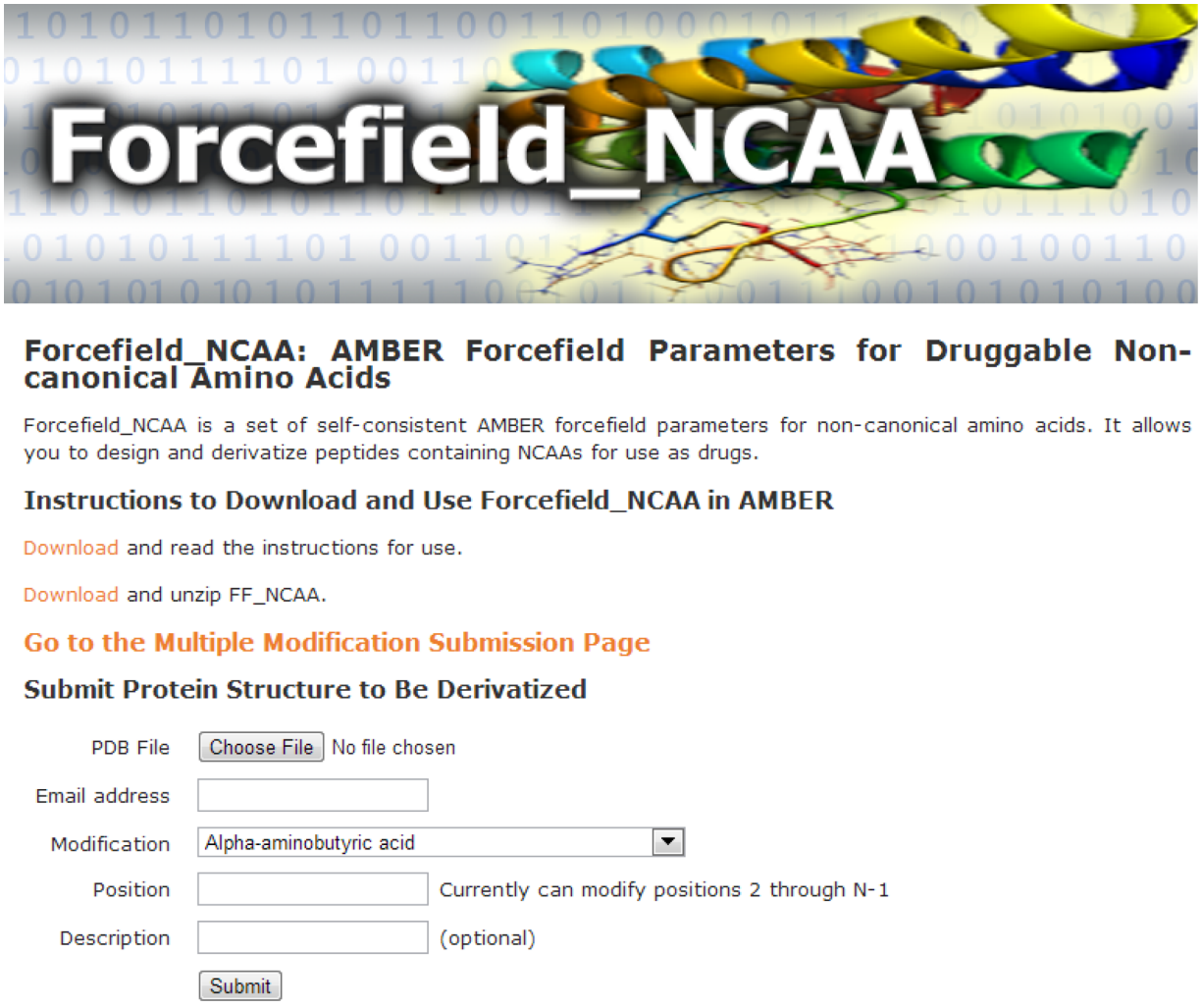

Figure 4. Web interface for the dissemination of Forcefield_NCAA. The web interface has static links to download and use Forcefield_NCAA in AMBER locally, as well as an interactive interface to make noncanonical amino acid substitutions and mutations to an input PDB structure. Screenshot taken April 25, 2013.

user will receive an e-mail indicating the structure's successful modification with a unique link to download their results. The user can visualize the modified and input structure using a Jmol applet integrated into the web interface. Additionally, the interface provides links to relevant information tabulated about the structures including the TMScore and[58] and RMSD between the structures, and the molecular-mechanics calculated energy of the structure. In addition, the topology and parameter files are generated for AMBER and are provided so that one can directly use them as input for further molecular dynamics simulation on the user's local computing systems. Disulfide bridges in the input structure are automatically detected and introduced by the web interface. The web interface will be useful to researchers aiming to interactively make site-specific noncanonical amino acid substitutions on a protein structure/complex and to perform subsequent binding calculations in AMBER locally.

METHODS

Procedure for Calculation and Derivation of Forcefield Parameters in Forcefield_NCAA. Quantum calculations to derive partial charges compatible with AMBER ff03 were performed consistent with the procedure of Duan and coworkers[51] for the 20 natural amino acids. The ff03 methodology was chosen due to the noncanonical amino acids having multiple R-groups attached to the C_α or substitutions such as methylation on the backbone nitrogen. Therefore, the consensus fixed-backbone charges in other AMBER fixed-charge forcefields would not be applicable.[50] The choices for NCAAs chosen to be parametrized were based on those found in the literature to enhance the binding affinity of a peptide to a receptor protein, α,α-disubstituted modified amino acids, N-methylated amino acids, and β-amino acids. The procedure used is shown in Figure 5 and is adapted from the procedure we developed to derive parameters in Forcefield_PTM[50] for parametrizing frequently occurring post-translational modifications.

In the first step, structures of each unnatural amino acid dipeptide were built using the MarvinSketch program.[59] Dipeptides are constructed to mimic the peptide backbone with a core amino acid with a preceding and subsequent amino acid. An acetyl group precedes the amino acid to be parametrized, with an N-methyl group following it in the form ACE-X-NME, where X is the amino acid to be parametrized. L-Amino acids were constructed, unless otherwise noted by designations of (R) or (S) for the disubstituted amino acids. In the second step, the distance geometry (**distgeom**)

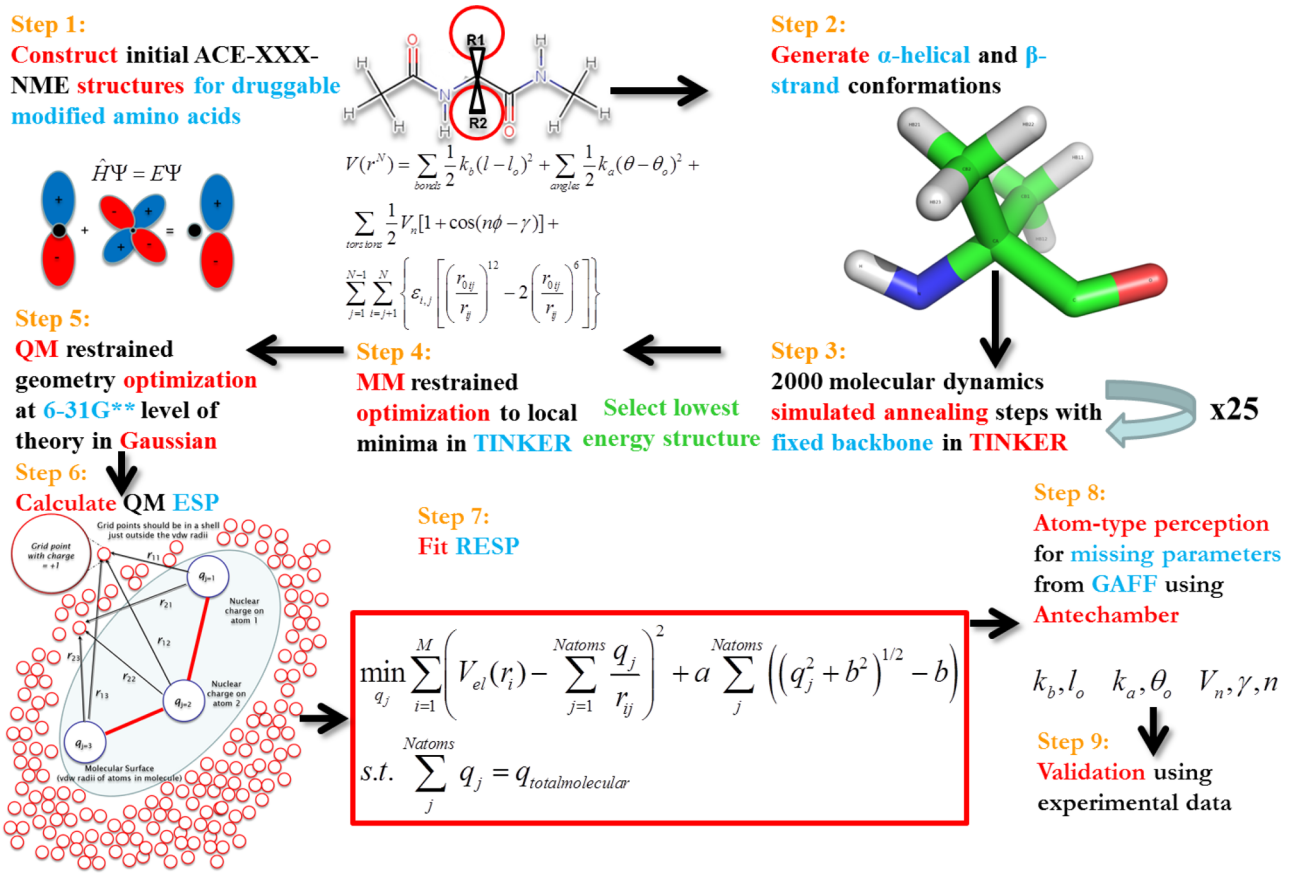

Figure 5. Automated framework for AMBER partial charge parametrization for noncanonical, α,α-disubstituted, β- and N-methylated amino acids. Adapted with permission from ref 50. Copyright 2013, American Chemical Society.

module in TINKER 5.1[60] is used to construct α-helix (ϕ = −60, ψ = −40) and β-strand (ϕ = −120, ψ = −140) conformers. In Step 3, through TINKER, utilizing the AMBER ff94[61] parameter set, and using restraints on the main-chain torsion angles, each conformer was subjected to 25 simulated annealing calculations (using the **anneal** routine with default parameters). T_i and T_f were 1000 K and 0 K in the annealing. 2000 steps of cooling are done in each simulation, employing a linear cooling protocol and a 1 fs time step. This procedure was performed to find suitable feasible points for subsequent detailed optimization at the quantum mechanical level. For both the helix and strand conformer, the lowest energy structure for each was minimized to the nearest local minima using the **optimize** routine, with a RMS gradient cutoff of 0.01. *Gaussian09*[62] was used to optimize (Step 5) each conformer at the HF/6-31G** level of theory, with restraints on the ϕ and ψ angles to preserve the backbone secondary structure. Single point energy calculations are next performed on the dipeptide structures using the density functional theory method and the B3LYP exchange and correlation functionals[63−65] and the cc-pVTZ[66] basis set. An ether-like organic solvent environment (ε = 4) was mimicked by applying the IEFPCM implicit solvent model,[67,68] as suggested by Duan.[51] The electrostatic potential (ESP) was calculated at a set of gridpoints defining the molecular surface in the solvent-accessible region around each optimized conformation at 1.4, 1.6, 1.8, and 2.0 times the vdw radii using the program DMS at a density of 0.5, yielding 2.5−2.8 points/Å^2.[69] The ESP values calculated from each conformation were next used as input to a two-stage RESP fit of the partial atomic charges using Antechamber in AmberTools 1.4.[70] In the RESP model, atoms are reasonably approximated as spherical points having fixed charges rather than as nuclei with shared electrons. Bond, angle, and dihedral force constants were perceived by matching atom types contained in the General Amber Forcefield (GAFF)[71] using Antechamber.[70] GAFF torsion parameters, when applied to post-translational modifications, were shown previously to be highly correlated with and reproduce the locations of local maxima/minima on the quantum mechanically calculated potential energy surface of key torsion angles, although their amplitudes needed refinement.[50] Subsequent refinement of key bonded parameters may be warranted but are not developed in this work due to the extreme computational cost involved and since the parameters developed herein are intended to be used mainly in a design context. This procedure was completed for a total of 147 diverse noncanonical amino acids spanning all amino acids except Proline. No new atom types were needed in the matching of force constants and equilibrium values. Further, in 99 of the 147 molecules parametrized, no parameters were utilized from GAFF since AMBER already had defined the parameters for all of the atom types for those noncanonical amino acids. The method described is similar to that described by Khoury et al.[50] with the changes being able to handle α,α-disubstituted and backbone modified amino acids. The parameters for noncanonical amino acids were next tested using binding calculations.

Testing the Parameters Using Approximate Binding Affinity and Binding Free Energy Calculations of 63 Compstatin Analogs. *Selection of System for Testing and Extraction of Data from the Literature.* We aimed to create

dx.doi.org/10.1021/sb400168u | ACS Synth. Biol. 2014, 3, 855−869

charge parameters for noncanonical amino acids that would be compatible with the existing AMBER ff03 forcefield parameters for natural amino acids. We focused on assessing whether the derived parameters can discriminate between active/inactive analogs of an inhibitor, since we expect the charge parameters derived to be used mainly in a protein design context. This approach is viable since there are sets of binding data available in the literature where others have experimentally incorporated noncanonical amino acids for various therapeutic applications.

The availability of (i) an experimentally solved structure for Compstatin variant E1 (the ligand) bound to human Complement component C3c[55] (the receptor) and (ii) an abundance of experimental binding and IC_{50} data available, and the observation that (iii) the ligand peptide is relatively rigid because of a disulfide bond that cyclizes it which limits the entropic contribution to the binding free energy, led us to focus our testing efforts on the Complement/Compstatin system. There are three pathways in the Complement system: the classical pathway, the lectin pathway, and the alternative pathway.[72] All three pathways converge on a single step where the key protein, C3 binds to C3 convertase and causes it to become cleaved into C3a and C3b (which contains C3c), which allows downstream events to occur leading to the membrane attack complex that can cleave cells. Compstatin binds to C3 and the C3 convertase, which blocks them from coming together and becoming cleaved.[73] Inhibiting their ability to bind together and cleave inhibits the activation of C3 and disrupts the formation of the membrane attack complex downstream. This is important as its improper activation has been linked to over 10 autoimmune, inflammation, and neurological disorders.[24,74−77]

Figure 6 shows a schematic diagram of Complement component C3c with the coordinates of the ligand peptide Compstatin variant E1 (Ac-ICVWQDWGAHRCT-NH2) bound. Since the region that Compstatin binds to C3c is confined and localized in one site, utilizing the entire C3c:Compstatin complex is not necessary. In addition, because of unresolved/missing residues in the crystal structure, and because of its large size (643 amino acids in the solved PDB structure), using the full structure of C3c only serves to complicate subsequent calculation complexities, extend simulation times, and potentially add unnecessary noise.[49,56,57] Therefore, residues F335 (macroglobulin domain 4,MG4) to D535 (MG5) were extracted from PDB: 2QKI and used in all subsequent calculations. Previous simulations to study this complex have shown that using these regions were sufficient for modeling the binding interface.[49,57]

All experimental binding data (IC_{50}'s) on Compstatin variants were tabulated from Magotti et al.,[52] Chiu et al.,[79] and Qu et al.[24] These data sets are denoted by structurekinetic, pharmacophore, and novel analogues, respectively, and are shown in Table 3. The data set included 47 analogues with IC_{50} < 200 μM, and 16 analogs with IC_{50} > 200 μM, as well as 31 analogues with IC_{50} < 20 μM and 32 analogs with IC_{50} > 20 μM. In terms of diversity, the data set included 23 noncanonical amino acid modifications, of which 11 were backbone N-methylations, 28 were natural amino acid substitutions, and 12 were deletions. There was no training done specific to this system in the derivation of the parameters for the NCAAs used. All subsequent results are based only on physical interactions derived from the physics governing the AMBER forcefield.

Screening Compstatin Analogs with Short Molecular Dynamics Simulations and Binding Calculations. The

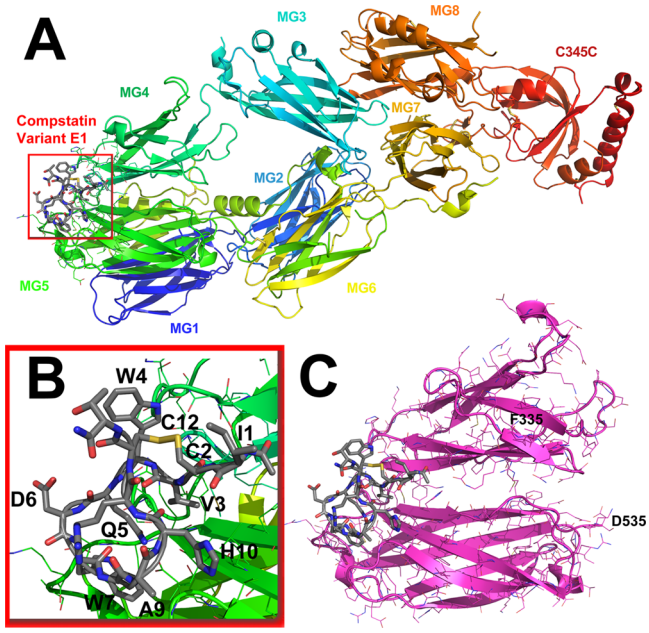

Figure 6. (A) Crystal structure of Compstatin Variant E1 bound to Complement component C3c (PDB: 2QKI). Each macroglobulin domain (MG) is denoted by color. (B) The region where modified amino acids are to be substituted in is shown in the inset. This is the interface that is being designed when making natural or noncanonical amino acid substitutions. A disulfide bridge cyclizes Compstatin between residues 2 and 12. (C) This is the full region all calculations will be performed on, beginning with F335 from MG4 to D535 on MG5 as labeled. The images are visualized in PyMOL.[78]

starting coordinates of variant E1 of Compstatin bound to Complement component C3c were taken from PDB: 2QKI. Each variant was constructed using the program **tleap** by stripping off the side-chains and substituting them with the new amino acid, natural or modified. Deletions were constructed by deleting the amino acids on the peptide chain. During the initial minimization the atoms moved to adjust for the deletions. The cysteine residues in the Compstatin variants were connected to form disulfide bridges in all simulations using the **bond** command in **tleap**. Acetyl and N-methyl blocking groups were added if they were present in the experimental analog.

The molecular dynamics and screening procedure used was done identically for each variant with AMBER11.[80] Partial charges compatible with AMBER ff03[51] derived in this work were used for all noncanonical amino acids. All simulations were performed with the generalized Born implicit solvent model of Onufriev[81,82] with a 16 Å nonbonded interaction cutoff. The surface energy term was activated and a salt concentration of 0.1 mol/L was used to account for charge screening. Structures were minimized with 600 steps of steepest descent followed by 400 steps of conjugate gradient minimization. The structures were next heated by rescaling the velocities in 6 stages with increments of 50 K from 0 K to 300 K over 30 ps and a 0.5 fs time step to heat the structures. The collision frequency γ was 5 ps^{-1}. Shake constraints were used to constrain all bonds between heavy atoms and hydrogens and reduce the number of degrees of freedom. Next, each C3c/Compstatin variant underwent a short 0.5 ns production simulation using a 1 fs time step at 300 K. Short (<1 ns) MD simulations with the ff03 charge model have previously been shown to give better performance in ranking

dx.doi.org/10.1021/sb400168u | *ACS Synth. Biol.* 2014, 3, 855−869

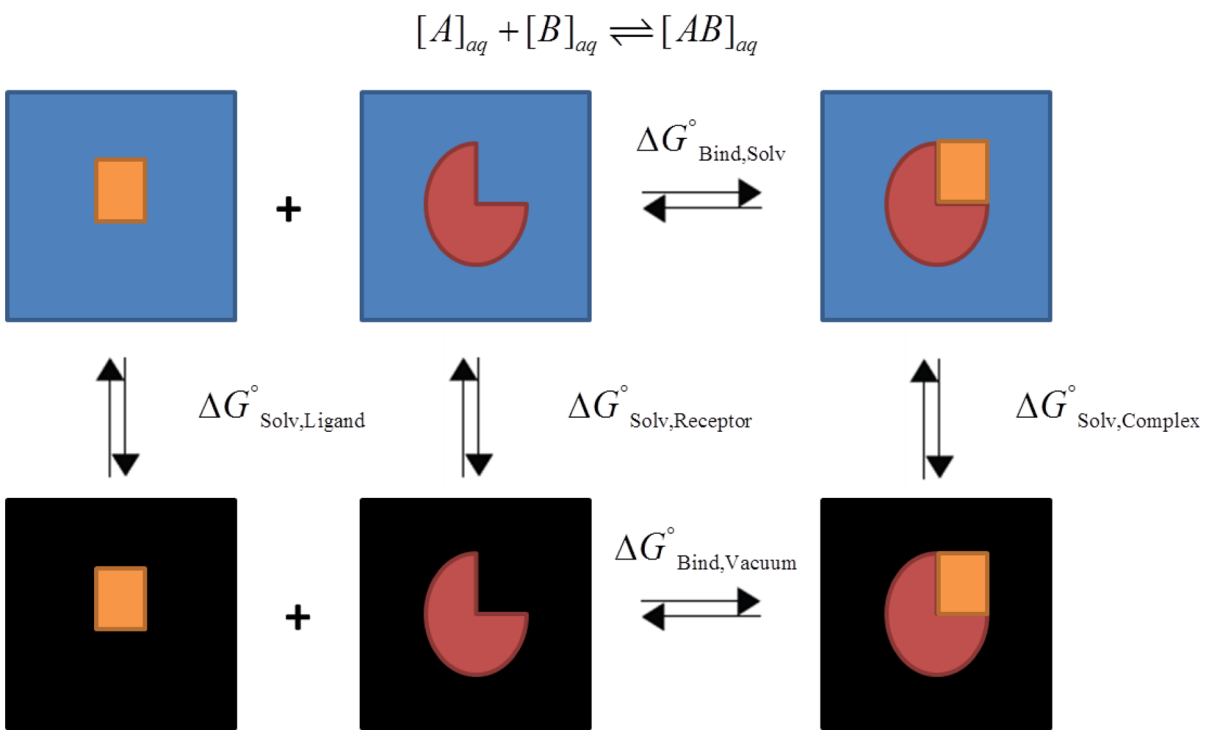

Figure 7. Thermodynamic cycle used to calculate the binding free energies. Ideally one can calculate the binding free energy for the association of [A] + [B] ⇌ [AB] directly in solvent. This calculation is expensive and contains much noise due to the contribution of the solvent. Therefore, a different approach was used exploiting a thermodynamic cycle that can calculate the same difference by utilizing the solvation free energies of the protein (receptor), peptide (ligand), and complex, with the binding energy calculated *in vacuo*.[87]

binding energies than longer simulations[83] and gave the best overall ranking results in an assessment of 5 AMBER forcefields (ff99, ff99SB, ff99SB-ILDN, ff03, and ff12SB) and 46 small molecules targeting 5 protein receptors.[84] No restraints were employed in any step of any simulation to strictly assess the suitability of the parameters to discriminate between active/inactive analogs of Compstatin.

Approximate Binding Affinity Calculations. Three independent simulations as described above were performed for the complex, the protein, and the peptide, respectively. One simulation of the protein was utilized to assess the contributions of the protein and to remove any variability from its contribution. Sixty three independent simulations of each complex and 63 independent simulations of each peptide were performed in isolation using the procedure described above. The derivation of the Approximate Binding Affinity (K^*) from statistical mechanics is described in the following.

The equilibrium of complex formation PL from a protein P and ligand L is defined as

$$\mathrm{P} + \mathrm{L} \rightleftharpoons \mathrm{PL} \tag{1}$$

Assuming a dilute mixture, one can assume ideal behavior. The Helmholtz free energy A can be related to the total partition function, Q in eq 2. Q is in turn a function of the individual partition functions q_i, where i is PL, P, L. This assumes independence of subsystems and that the particles are indistinguishable.

$$Q = \prod_{i=1}^{3} \frac{q_i^{N_i}}{N_i!} = \mathrm{e}^{-A/kT} \tag{2}$$

The chemical potential μ of species i is the partial derivative of the Helmholtz Free Energy A with respect to N_i, denoted in eq 3.

$$\mu_i = \left(\frac{\partial A}{\partial N_i}\right)_{T,V,N_j \neq N_i} = -kT\frac{\partial \ln Q}{\partial N_i} = -kT\ln\frac{q_i}{N_i}. \tag{3}$$

Equality of chemical potentials at equilibrium is denoted in eq 4.

$$\mu_{\mathrm{P}} + \mu_{\mathrm{L}} = \mu_{\mathrm{PL}} \tag{4}$$

Next, substituting eq 3 into eq 4 and rearranging yields.

$$\frac{q_{\mathrm{PL}}}{q_{\mathrm{P}}q_{\mathrm{L}}} = \frac{N_{\mathrm{PL}}}{N_{\mathrm{P}}N_{\mathrm{L}}} \tag{5}$$

q_i is a product of the translational (q_t), rotational (q_r), and vibrational (q_v) partition functions. Since q_t is only a function of the coordinates x, y, and z, it integrates out to a volume V, leaving $q_i = V * q_i'(T)$. $q_i'(T)$ is the rotational and vibrational partition functions, which is what is approximated by evaluation of E_{intra} during the snapshots sampled over the course of a molecular dynamics trajectory. This is shown in eq 6.

$$\begin{aligned} q_i(V, T) &= q_t q_v q_r = \int \dots \int \mathrm{d}\mathbb{N}\, \mathrm{e}^{-E_{\text{intra}}/kT} \\ &= V \int \dots \int \mathrm{d}\mathbb{N}'\, \mathrm{e}^{-E_{\text{intra}}/kT} = V q_v q_r = V q_i'(T) \end{aligned} \tag{6}$$

Next, the volume term can be taken out of each partition function and therefore the ratio of the partition functions equals the ratio of concentrations (since N_i/V_i is a concentration). $K^* = K_A$ when the intrapartition functions (q_r and q_v) are exactly calculated.

dx.doi.org/10.1021/sb400168u | *ACS Synth. Biol.* 2014, 3, 855−869

$$\frac{q'_{PL}}{q'_P q'_L} = \frac{[PL]}{[P][L]} = K_A = \frac{\sum_{b\in B} e^{-E_b/kT}}{\sum_{f\in F} e^{-E_f/kT} \sum_{l\in L} e^{-E_l/kT}} = K^* \quad (7)$$

Currently, it is not possible to compute exact partition functions for a complex molecular species due to the inability to integrate an exact energy function over the molecule's entire conformational space.[85] Therefore, we approximate the partition functions as the sampled space of a molecular dynamics trajectory scored with the AMBER potential energy function.

This derivation is based on an initial derivation by Lilien et al.[85] using rotamerically based ensembles with modifications resulting from a personal communication between Dr. Meghan Bellows Peterson and Professor Pablo G. Debenedetti. Using the ratios of the partition function of the complex, peptide, and protein, the Approximate Binding Affinity, K^* was calculated and placed in a rank ordered list from highest to lowest, which would correspond to the largest to smallest predicted association affinity. The Jacobi logarithm was used to handle numerical overflows that can be caused by summing exponential terms.[86]

Binding Free Energy Calculations. Binding free energies were calculated using the states produced over the time course of each of the 63 molecular dynamics simulations of the complex. These were calculated to test the forcefield parameters and also to compare its predictive ability to the K^*. In the approximate binding affinity, independent simulations of the peptide, protein, and complex are performed. In the binding free energy calculation, only one simulation of the complex is required. The binding free energy is calculated as in eq 8, utilizing the thermodynamic cycle denoted in Figure 7.

$$\Delta G^\circ_{Bind,Solv} = \Delta G^\circ_{Bind,Vacuum} + \Delta G^\circ_{Solv,Complex} - (\Delta G^\circ_{Solv,Ligand} + \Delta G^\circ_{Solv,Receptor}) \quad (8)$$

Tamamis et al., using the CHARMM[54] suite of tools, showed MM-GBSA was able to show the difference in binding Compstatin in complex with human versus rat C3c[56] and mouse C3c.[57] Tamamis et al. further showed MM-GBSA was helpful in discriminating potential analogs for experimental testing.[49] Based on these previous findings, it is clear that MM-GBSA can be used to study the Compstatin/C3c system. Therefore, in this study, binding free energies were calculated using the MM-GBSA module[87] in AMBER11 complemented by the charge parameters for the noncanonical amino acids introduced in this work.

For this system, we assume that the entropic contribution due to the binding free energy is small since the ligand's structure is relatively rigid due to the disulfide bridges (the maximum C_α RMSD between analogs W4(OMW)A9, W4A9, and native Compstatin was 1.38 at the end of the simulation). The entropic contribution, which can be calculated through a normal-mode analysis, can have a large uncertainty.[80] Given that we expect the Compstatin analogs to have similar entropies due to their cyclic nature and being bound to the same binding pocket of C3c, and because of the expected large error, the entropic contribution in the calculation was ignored. This "one-trajectory" approximation where we assume similar structure in the bound and unbound state is reasonable and has been applied elsewhere[49,53] and also has been compared to the results of a "three-trajectory" approximation for this system.[56] Using the "one-trajectory" approximation, all of the bonded terms (bonds, angles, torsions) cancel out in the evaluation of the binding free energies, leaving only nonbonded terms, of which the electrostatic component is a significant contributor.

Construction of Receiver Operating Characteristic Curves. After the approximate binding affinity and binding free energies were calculated for each variant of Compstatin following the procedure described above, the values were rank ordered from most favorable to least favorable. For K^*, this was largest to smallest, and for $\Delta G^\circ_{Bind,Solv}$, this was smallest to largest. Receiver operating characteristic (ROC) curves were constructed based on the rank-ordered lists of the analogs. Two cutoff values of IC_{50} values defining active and inactive were chosen. The first cutoff was 20 M, which corresponded to an even split between active and inactive in the data set. That is, analogs with IC_{50} values < 20 μM were considered active. Similarly, a cutoff of 200 μM was chosen to perform the analysis with a less stringent cutoff of active/inactive. These values as cutoffs were determined based on the fact that the most active Compstatin analog in Table 3 is Ac-ICV(OMW)-QDWGAHRCT-NH2,[88] which has an IC_{50} of 0.21 μM. The axes on the ROC curve correspoμnd to the True Positive Rate (Sensitivity) vs the False Positive Rate (1-Specificity). The ROC curve constructed aimed to find how many of the most favorable analogs by calculated approximate binding affinity or binding free energy were experimentally active when rank-ordered. In a virtual screen, this is often one of the first steps in design: to assess whether a particular ligand will bind to its target favorably, and ranking the affinity of a ligand to the targeted receptor. Sensitivity and specificity are defined as.

$$\text{sensitivity} = \frac{TP}{TP + FN} \quad \text{specificity} = \frac{TN}{TN + FP} \quad (9)$$

where TP, FP, TN, and FN stand for true/false positives/negatives, respectively.

Additional Simulations for Analysis of Interaction Free Energies of Compstatin Derivatives and C3 Residue Pairs. Three biologically relevant complexes containing derivatives of Compstatin (Sequence 11: Ac-ICV(OMW)-QDWGAHRCT-NH2, Sequence 23: Ac-ICVWQDW-GAHRCT-NH2, and Sequence 53: ICVVQDWGHHRCT in Table 3) were assessed for their interactions through multiple longer-time molecular dynamics simulations. Four independent trajectories were performed for each complex. Each of the four trajectories for each complex were appended together for subsequent analysis. The starting complex structures were constructed and minimized as described previously deriving from PDB: 2QKI. The complexes were heated stepwise from 0 to 300K over 30 ps using restraints on all backbone atoms with a force constant of 10 kcal/(mol·Å^2). The complexes were carefully equilibrated in 3 stages; each stage was run for 200 ps. In the first stage, all atoms were restrained with a force constant of 5.0 kcal/(mol·Å^2) for 200 ps. In the second stage, all backbone atoms outside of the binding pocket were constrained (residues 335−343, 350−387, 394−453, 463−487, 493−535), and all atoms in the binding pocket were constrained with a force constant of 5.0 kcal/(mol·Å^2). In the final stage, all backbone atoms outside of the binding pocket were constrained and all atoms in the binding pocket were constrained with a force constant of 1.5 kcal/(mol·Å^2). After equilibration, four independent 10 ns production simulations were performed for each complex. These simulations were used to produce maps of

dx.doi.org/10.1021/sb400168u | ACS Synth. Biol. 2014, 3, 855−869

residue−residue polar and nonpolar interaction free energies to identify key energetic interactions important for binding through the simulation trajectories.

The interaction free energies between two residues (R and R') were computed by the relation:

$$\Delta G^{\text{inte}}_{RR'} = \underbrace{\sum_{i\in R}\sum_{j\in R'}\left(E^{\text{Coul}}_{ij} + E^{\text{GB}}_{ij}\right)}_{\Delta G^{\text{polar}}_{RR'}} + \underbrace{\sum_{i\in R}\sum_{j\in R'} E^{\text{vdW}}_{ij} + \sigma\sum_{i\in R,R'}\Delta SASA_i}_{\Delta G^{\text{non polar}}_{RR'}} \quad (10)$$

for each of the 3 Compstatin variants evaluated. The first and second group of terms on the right-hand side of eq 10 describe polar and nonpolar interactions between R and R'. In the calculations, R corresponds to a residue on Compstatin and R' corresponds to a residue on C3c. The details of the calculation have been presented previously.[49,53,56,57] For each complex, 4000 frames over the 40 ns total simulation time were evaluated for their average interaction free energies using a spacing of 10 ps per frame.

■ ASSOCIATED CONTENT

Supporting Information

(1) Table containing the raw calculated binding affinities of different Compstatin variants. (2) Instructions for importing new parameters into AMBER. (3) Explanation of the contents of the forcefield parameter file. (4) Images and atom namings of each parametrized noncanonical amino acid grouped by scaffold residue. (5) Forcefield parameters for each non-canonical amino acid grouped by scaffold residue. (6) The full pairwise residue−residue analysis of interaction energy contributions for 3 important analogs of Compstatin. (7) Zip file containing the Forcefield parameters in AMBER formats directly importable into AMBER. This material is available free of charge via the Internet at http://pubs.acs.org.

■ AUTHOR INFORMATION

Corresponding Author

*Phone: 609-258-4595. Fax: 609-258-0211. E-mail: floudas@titan.princeton.edu.

Author Contributions

G.A.K. and C.A.F. conceived the project. G.A.K. and J.S. contributed to the source code enabling the calculation of the parameters. G.A.K. and A.V. calculated and compiled the partial charges. J.S., C.A.K., G.A.K. contributed to the construction of the ROC curves. G.A.K. performed the simulations and constructed the ROC curves. G.A.K., J.S., C.A.K., and C.A.F. analyzed the ROC curves. P.T. and G.A.K. constructed the interaction maps and analyzed the simulation results. G.A.K. created the web interface. G.A.K., P.T., and C.A.F. wrote the manuscript. All authors have read and approved the manuscript.

Notes

The authors declare no competing financial interest.

■ ACKNOWLEDGMENTS

C.A.F. acknowledges support from the National Institutes of Health (R01GM052032) and the National Science Foundation. G.A.K. is grateful for support by a National Science Foundation Graduate Research Fellowship under grant No. DGE-1148900. The authors gratefully acknowledge that the calculations reported in this paper were performed at the TIGRESS high performance computing center at Princeton University which is supported by the Princeton Institute for Computational Science and Engineering (PICSciE) and the Princeton University Office of Information Technology. The authors are grateful to Eric First for expert help with making the webtool. We are grateful to Dr. Meghan Bellows Peterson and Professor Pablo G. Debenedetti for helpful discussions.

■ ABBREVIATIONS

μM, micromolar concentration; $\mathbb{N}$, all degrees of freedom; $\mathbb{N}'$, all the degrees of freedom minus the translational degrees of freedom; E_{intra}, the intramolecular energy of a system interacting with itself; Q, the total partition function; q_i', the partition function over the internal degrees of freedom; B, the set of bound configurations; F, the set of free protein configurations; L, the set of free ligand peptide configurations; K^*, the approximate binding affinity; K_A, the binding equilibrium constant for the association reaction P + L ⇌ PL

■ REFERENCES

(1) Wang, J., and Hou, T. (2011) Recent advances on aqueous solubility prediction. *Comb. Chem. High Throughput Screening 14*, 328−338.

(2) Andrade, C. H., Pasqualoto, K. F. M., Ferreira, E. I., and Hopfinger, A. J. (2009) Rational design and 3D-pharmacophore mapping of 5′-thiourea-substituted α-thymidine analogues as mycobacterial TMPK inhibitors. *J. Chem. Inf. Model. 49*, 1070−1078.

(3) Vlieghe, P., Lisowski, V., Martinez, J., and Khrestchatisky, M. (2010) Synthetic therapeutic peptides: Science and market. *Drug Discovery Today 15*, 40−56.

(4) Craik, D. J., Fairlie, D. P., Liras, S., and Price, D. (2013) The future of peptide-based drugs. *Chem. Biol. Drug Des. 81*, 136−147.

(5) Adessi, C., and Soto, C. (2002) Converting a peptide into a drug: Strategies to improve stability and bioavailability. *Curr. Med. Chem. 9*, 963−978.

(6) Miller, S. M., Simon, R. J., Ng, S., Zuckermann, R. N., Kerr, J. M., and Moos, W. H. (1995) Comparison of the proteolytic susceptibilities of homologous L-amino acid, D-amino acid, and N-substituted glycine peptide and peptoid oligomers. *Drug Dev. Res. 35*, 20−32.

(7) Khoury, G. A., Baliban, R. C., and Floudas, C. A. (2011) Proteome-wide post-translational modification statistics: Frequency analysis and curation of the SWISS-PROT database. *Sci. Rep. 1*, 1−5.

(8) Bairoch, A., and Apweiler, R. (2000) The SWISS-PROT protein sequence database and its supplement TrEMBL in 2000. *Nucleic Acids Res. 28*, 45−48.

(9) Khoury, G. A., Smadbeck, J., Kieslich, C. A., and Floudas, C. A. (2013) Protein folding and *de novo* protein design for biotechnological applications. *Trends Biotechnol.*, DOI: 10.1016/j.tibtech.2013.10.008.

(10) Walsh, C. T. (2006) *Posttranslational Modification of Proteins: Expanding Nature's Inventory*; Roberts and Co. Publishers, Englewood, CO, pp xxi, 490.

(11) Merrifield, R. B. (1963) Solid phase peptide synthesis. I. The synthesis of a tetrapeptide. *J. Am. Chem. Soc. 85*, 2149−2154.

(12) Chalker, J. M., and Davis, B. G. (2010) Chemical mutagenesis: selective post-expression interconversion of protein amino acid residues. *Curr. Opin. Chem. Biol. 14*, 781−789.

(13) Chalker, J. M., Bernardes, G. J. L., and Davis, B. G. (2011) A "tag-and-modify" approach to site-selective protein modification. *Acc. Chem. Res. 44*, 730−741.

(14) Johnson, J. A., Lu, Y. Y., Van Deventer, J. A., and Tirrell, D. A. (2010) Residue-specific incorporation of non-canonical amino acids

into proteins: Recent developments and applications. *Curr. Opin. Chem. Biol. 14*, 774−780.
(15) Neumann, H., Wang, K., Davis, L., Garcia-Alai, M., and Chin, J. W. (2010) Encoding multiple unnatural amino acids via evolution of a quadruplet-decoding ribosome. *Nature 464*, 441−444.
(16) Wang, L., Xie, J., and Schultz, P. G. (2006) Expanding the genetic code. *Annu. Rev. Biophys. Biomol. Struct. 35*, 225−249.
(17) Watanabe, T., Muranaka, N., and Hohsaka, T. (2008) Four-base codon-mediated saturation mutagenesis in a cell-free translation system. *J. Biosci. Bioeng. 105*, 211−215.
(18) Mapelli, C., et al. (2009) Eleven amino acid glucagon-like peptide-1 receptor agonists with antidiabetic activity. *J. Med. Chem. 52*, 7788−7799.
(19) Sievers, S. A., Karanicolas, J., Chang, H. W., Zhao, A., Jiang, L., Zirafi, O., Stevens, J. T., Munch, J., Baker, D., and Eisenberg, D. (2011) Structure-based design of non-natural amino-acid inhibitors of amyloid fibril formation. *Nature 475*, 96−100.
(20) Bakos, K., Havass, J., Fülöp, F., Gera, L., Stewart, J. M., Falkay, G., and Tóth, G. K. (2001) Synthesis and receptor binding of oxytocin analogs containing conformationally restricted amino acids. *Lett. Pept. Sci. 8*, 35−40.
(21) Tamamura, H., Hiramatsu, K., Kusano, a. S., Terakubo, S., Yamamoto, N., Trent, J. O., Wang, Z., Peiper, S. C., Nakashima, H., Otaka, A., and Fujii, N. (2003) Synthesis of potent CXCR4 inhibitors possessing low cytotoxicity and improved biostability based on T140 derivatives. *Org. Biomol. Chem. 1*, 3656−3662.
(22) Kokubu, T., Hiwada, K., Murakami, E., Imamura, Y., Matsueda, R., Yabe, Y., Koike, H., and Iijima, Y. (1985) Highly potent and specific inhibitors of human renin. *Hypertension 7*, I8−11.
(23) Mallik, B., Katragadda, M., Spruce, L. A., Carafides, C., Tsokos, C. G., Morikis, D., and Lambris, J. D. (2005) Design and NMR characterization of active analogues of compstatin containing non-natural amino acids. *J. Med. Chem. 48*, 274−286.
(24) Qu, H., Magotti, P., Ricklin, D., Wu, E. L., Kourtzelis, I., Wu, Y.-Q., Kaznessis, Y. N., and Lambris, J. D. (2011) Novel analogues of the therapeutic complement inhibitor compstatin with significantly improved affinity and potency. *Mol. Immunol. 48*, 481−489.
(25) Leaver-Fay, A., et al. (2011) Rosetta3 an object-oriented software suite for the simulation and design of macromolecules. *Methods Enzymol. 487*, 545−574.
(26) Correia, B. E., et al. (2010) Computational design of epitope-scaffolds allows induction of antibodies specific for a poorly immunogenic HIV vaccine epitope. *Structure 18*, 1116−1126.
(27) Fleishman, S. J., Whitehead, T. A., Ekiert, D. C., Dreyfus, C., Corn, J. E., Strauch, E.-M., Wilson, I. A., and Baker, D. (2011) Computational design of proteins targeting the conserved stem region of influenza hemagglutinin. *Science 332*, 816−821.
(28) Whitehead, T. A., Chevalier, A., Song, Y., Dreyfus, C., Fleishman, S. J., De Mattos, C., Myers, C. A., Kamisetty, H., Blair, P., Wilson, I. A., and Baker, D. (2012) Optimization of affinity, specificity, and function of designed influenza inhibitors using deep sequencing. *Nat. Biotechnol. 30*, 543−548.
(29) Jiang, L., Althoff, E. A., Clemente, F. R., Doyle, L., Rothlisberger, D., Zanghellini, A., Gallaher, J. L., Betker, J. L., Tanaka, F., Barbas, I., Carlos, F., Hilvert, D., Houk, K. N., Stoddard, B. L., and Baker, D. (2008) *De novo* computational design of retro-aldol enzymes. *Science 319*, 1387−1391.
(30) Richter, F., et al. (2012) Computational design of catalytic dyads and oxyanion holes for ester hydrolysis. *J. Am. Chem. Soc. 134*, 16197−16206.
(31) Althoff, E. A., Wang, L., Jiang, L., Giger, L., Lassila, J. K., Wang, Z., Smith, M., Hari, S., Kast, P., Herschlag, D., Hilvert, D., and Baker, D. (2012) Robust design and optimization of retroaldol enzymes. *Protein Sci. 21*, 717−726.
(32) Siegel, J. B., Zanghellini, A., Lovick, H. M., Kiss, G., Lambert, A. R., St.Clair, J. L., Gallaher, J. L., Hilvert, D., Gelb, M. H., Stoddard, B. L., Houk, K. N., Michael, F. E., and Baker, D. (2010) Computational design of an enzyme catalyst for a stereoselective bimolecular Diels−Alder reaction. *Science 329*, 309−313.
(33) Rothlisberger, D., Khersonsky, O., Wollacott, A. M., Jiang, L., DeChancie, J., Betker, J., Gallaher, J. L., Althoff, E. A., Zanghellini, A., Dym, O., Albeck, S., Houk, K. N., Tawfik, D. S., and Baker, D. (2008) Kemp elimination catalysts by computational enzyme design. *Nature 453*, 190−195.
(34) Eiben, C. B., Siegel, J. B., Bale, J. B., Cooper, S., Khatib, F., Shen, B. W., Players, F., Stoddard, B. L., Popovic, Z., and Baker, D. (2012) Increased Diels-Alderase activity through backbone remodeling guided by Foldit players. *Nat. Biotechnol. 30*, 190−192.
(35) Saraf, M. C., Moore, G. L., Goodey, N. M., Cao, V. Y., Benkovic, S. J., and Maranas, C. D. (2006) IPRO: an iterative computational protein library redesign and optimization procedure. *Biophys. J. 90*, 4167−4180.
(36) Khoury, G. A., Fazelinia, H., Chin, J. W., Pantazes, R. J., Cirino, P. C., and Maranas, C. D. (2009) Computational design of *Candida boidinii* xylose reductase for altered cofactor specificity. *Protein Sci. 18*, 2125−2138.
(37) Renfrew, P. D., Choi, E. J., Bonneau, R., and Kuhlman, B. (2012) Incorporation of noncanonical amino acids into Rosetta and use in computational protein−peptide interface design. *PLoS One 7*, e32637.
(38) Petrov, D., Margreitter, C., Grandits, M., Oostenbrink, C., and Zagrovic, B. (2013) A systematic framework for molecular dynamics simulations of protein post-translational modifications. *PLoS Comput. Biol. 9*, e1003154.
(39) Margreitter, C., Petrov, D., and Zagrovic, B. (2013) Vienna-PTM web server: A toolkit for MD simulations of protein post-translational modifications. *Nucleic Acids Res. 41*, W422−W426.
(40) Klepeis, J. L., Floudas, C. A., Morikis, D., Tsokos, C. G., Argyropoulos, E., Spruce, L., and Lambris, J. D. (2003) Integrated computational and experimental approach for lead optimization and design of compstatin variants with improved activity. *J. Am. Chem. Soc. 125*, 8422−8423.
(41) Klepeis, J. L., Floudas, C. A., Morikis, D., Tsokos, C. G., and Lambris, J. D. (2004) Design of peptide analogues with improved activity using a novel *de novo* protein design approach. *Ind. Eng. Chem. Res. 43*, 3817−3826.
(42) Bellows, M. L., Taylor, M. S., Cole, P. A., Shen, L., Siliciano, R. F., Fung, H. K., and Floudas, C. A. (2010) Discovery of entry inhibitors for HIV-1 via a new *de novo* protein design framework. *Biophys. J. 99*, 3445−3453.
(43) Bellows, M. L., Fung, H. K., Taylor, M. S., Floudas, C. A., Lopez de Victoria, A., and Morikis, D. (2010) New compstatin variants through two *de novo* protein design frameworks. *Biophys. J. 98*, 2337−2346.
(44) Fung, H. K., Floudas, C. A., Taylor, M. S., Zhang, L., and Morikis, D. (2008) Toward full-sequence *de novo* protein design with flexible templates for human *β*-defensin-2. *Biophys. J. 94*, 584−599.
(45) Bellows-Peterson, M. L., Fung, H. K., Floudas, C. A., Kieslich, C. A., Zhang, L., Morikis, D., Wareham, K. J., Monk, P. N., Hawksworth, O. A., and Woodruff, T. M. (2012) *De novo* peptide design with C3a receptor agonist and antagonist activities: Theoretical predictions and experimental validation. *J. Med. Chem. 55*, 4159−4168.
(46) Smadbeck, J., Peterson, M. B., Khoury, G. A., Taylor, M. S., and Floudas, C. A. (2013) Protein WISDOM: A workbench for in silico *de novo* design of biomolecules. *J. Visualized Exp.*, e50476.
(47) Lopez de Victoria, A., Gorham, R. D., Bellows-Peterson, M. L., Ling, J., Lo, D. D., Floudas, C. A., and Morikis, D. (2011) A new generation of potent complement inhibitors of the compstatin family. *Chem. Biol. Drug Des. 77*, 431−440.
(48) Bellows, M. L., and Floudas, C. A. (2010) Computational methods for *de novo* protein design and its applications to the human immunodeficiency virus 1, purine nucleoside phosphorylase, ubiquitin specific protease 7, and histone demethylases. *Curr. Drug Targets 11*, 264−278.
(49) Tamamis, P., López de Victoria, A., Gorham, R. D., Bellows-Peterson, M. L., Pierou, P., Floudas, C. A., Morikis, D., and Archontis, G. (2012) Molecular dynamics in drug design: New generations of compstatin analogs. *Chem. Biol. Drug Des. 79*, 703−718.

(50) Khoury, G. A., Thompson, J. P., Smadbeck, J., Kieslich, C. A., and Floudas, C. A. (2013) Forcefield_PTM: *Ab initio* charge and AMBER forcefield parameters for frequently occurring post-translational modifications. *J. Chem. Theory Comput. 9*, 5653−5674.
(51) Duan, Y., Wu, C., Chowdhury, S., Lee, M. C., Xiong, G., Zhang, W., Yang, R., Cieplak, P., Luo, R., Lee, T., Caldwell, J., Wang, J., and Kollman, P. (2003) A point-charge force field for molecular mechanics simulations of proteins based on condensed-phase quantum mechanical calculations. *J. Comput. Chem. 24*, 1999−2012.
(52) Magotti, P., Ricklin, D., Qu, H., Wu, Y.-Q., Kaznessis, Y. N., and Lambris, J. D. (2009) Structure−kinetic relationship analysis of the therapeutic complement inhibitor compstatin. *J. Mol. Recognit. 22*, 495−505.
(53) Gorham, R. D., Jr, Forest, D. L., Tamamis, P., López de Victoria, A., Kraszni, M., Kieslich, C. A., Banna, C. D., Bellows-Peterson, M. L., Larive, C. K., Floudas, C. A., Archontis, G., Johnson, L. V., and Morikis, D. (2013) Novel compstatin family peptides inhibit complement activation by drusen-like deposits in human retinal pigmented epithelial cell cultures. *Exp. Eye Res. 116C*, 96−108.
(54) Brooks, B. R., et al. (2009) CHARMM: The biomolecular simulation program. *J. Comput. Chem. 30*, 1545−1614.
(55) Janssen, B. J. C., Halff, E. F., Lambris, J. D., and Gros, P. (2007) Structure of compstatin in complex with complement component C3c reveals a new mechanism of complement inhibition. *J. Biol. Chem. 282*, 29241−29247.
(56) Tamamis, P., Morikis, D., Floudas, C. A., and Archontis, G. (2010) Species specificity of the complement inhibitor compstatin investigated by all-atom molecular dynamics simulations. *Proteins: Struct., Funct., Bioinf. 78*, 2655−2667.
(57) Tamamis, P., Pierou, P., Mytidou, C., Floudas, C. A., Morikis, D., and Archontis, G. (2011) Design of a modified mouse protein with ligand binding properties of its human analog by molecular dynamics simulations: The case of C3 inhibition by compstatin. *Proteins: Struct., Funct., Bioinf. 79*, 3166−3179.
(58) Zhang, Y., and Skolnick, J. (2005) TM-align: A protein structure alignment algorithm based on the TM-score. *Nucleic Acids Res. 33*, 2302−2309.
(59) *MarvinSketch*, version 6.0.3; (2010) ChemAxon, Budapest, Hungary.
(60) *TINKER*, version 5.0; (2010) Washington University, St. Louis, MO.
(61) Cornell, W. D., Cieplak, P., Bayly, C. I., Gould, I. R., Merz, K. M., Ferguson, D. M., Spellmeyer, D. C., Fox, T., Caldwell, J. W., and Kollman, P. A. (1995) A second generation force field for the simulation of proteins, nucleic acids, and organic molecules. *J. Am. Chem. Soc. 117*, 5179−5197.
(62) Frisch, M. J. et al. (2004) *Gaussian 03*, Revision C.02; Gaussian Inc., Wallingford, CT.
(63) Lee, C., Yang, W., and Parr, R. G. (1988) Development of the Colle−Salvetti correlation-energy formula into a functional of the electron density. *Phys. Rev. B 37*, 785.
(64) Miehlich, B., Savin, A., Stoll, H., and Preuss, H. (1989) Results obtained with the correlation energy density functionals of Becke and Lee, Yang, and Parr. *Chem. Phys. Lett. 157*, 200−206.
(65) Becke, A. D. (1993) Density-functional thermochemistry. III. The role of exact exchange. *J. Chem. Phys. 98*, 5648−5652.
(66) Kendall, R. A., Thom H. Dunning, J., and Harrison, R. J. (1992) Electron affinities of the first-row atoms revisited. Systematic basis sets and wave functions. *J. Chem. Phys. 96*, 6796−6806.
(67) Mennucci, B., Cammi, R., and Tomasi, J. (1999) Analytical free energy second derivatives with respect to nuclear coordinates: Complete formulation for electrostatic continuum solvation models. *J. Chem. Phys. 110*, 6858−6870.
(68) Tomasi, J., Mennucci, B., and Cances, E. (1999) The IEF version of the PCM solvation method: An overview of a new method addressed to study molecular solutes at the QM *ab initio* level. *J. Mol. Struct.: THEOCHEM 464*, 211−226.
(69) Richards, F. M. (1977) Areas, Volumes, Packing, and Protein Structure. *Annu. Rev. Biophys. Bioeng. 6*, 151−176.
(70) Wang, J., Wang, W., Kollman, P. A., and Case, D. A. (2006) Automatic atom type and bond type perception in molecular mechanical calculations. *J. Mol. Graph. Model. 25*, 247−260.
(71) Wang, J., Wolf, R. M., Caldwell, J. W., Kollman, P. A., and Case, D. A. (2004) Development and testing of a general Amber force field. *J. Comput. Chem. 25*, 1157−1174.
(72) Janeway, C. A., Travers, P., Walport, M., and Shlomchik, M. J. (2001) *Immunobiology*; Garland Science, New York.
(73) Sahu, A., Morikis, D., and Lambris, J. D. (2003) Compstatin, a peptide inhibitor of complement, exhibits species-specific binding to complement component C3. *Mol. Immunol. 39*, 557−566.
(74) Kovacs, G. G., Gasque, P., Ströbel, T., Lindeck-Pozza, E., Strohschneider, M., Ironside, J. W., Budka, H., and Guentchev, M. (2004) Complement activation in human prion disease. *Neurobiol. Dis. 15*, 21−28.
(75) Java, A., Atkinson, J., and Salmon, J. (2013) Defective complement inhibitory function predisposes to renal disease. *Annu. Rev. Med. 64*, 307−324.
(76) Ricklin, D., and Lambris, J. D. (2013) Complement in immune and inflammatory disorders: Therapeutic interventions. *J. Immunol. 190*, 3839−3847.
(77) Rensen, S. S., Slaats, Y., Driessen, A., Peutz-Kootstra, C. J., Nijhuis, J., Steffensen, R., Greve, J. W., and Buurman, W. A. (2009) Activation of the complement system in human nonalcoholic fatty liver disease. *Hepatology 50*, 1809−1817.
(78) *PyMOL*, version 1.3; Delano Scientific LLC, 2008.
(79) Chiu, T.-L., Mulakala, C., Lambris, J. D., and Kaznessis, Y. N. (2008) Development of a new pharmacophore model that discriminates active compstatin analogs. *Chem. Biol. Drug Des. 72*, 249−256.
(80) Case, D. A. et al. (2010) *Amber 11*, University of California, San Francisco.
(81) Onufriev, A., Bashford, D., and Case, D. A. (2000) Modification of the generalized Born Model suitable for macromolecules. *J. Phys. Chem. B 104*, 3712−3720.
(82) Onufriev, A., Bashford, D., and Case, D. A. (2004) Exploring protein native states and large-scale conformational changes with a modified generalized born model. *Proteins: Struct., Funct., Bioinf. 55*, 383−394.
(83) Hou, T., Wang, J., Li, Y., and Wang, W. (2011) Assessing the performance of the MM/PBSA and MM/GBSA methods. 1. The accuracy of binding free energy calculations based on molecular dynamics simulations. *J. Chem. Inf. Model. 51*, 69−82.
(84) Xu, L., Sun, H., Li, Y., Wang, J., and Hou, T. (2013) Assessing the performance of MM/PBSA and MM/GBSA methods. 3. The impact of force fields and ligand charge models. *J. Phys. Chem. B 117*, 8408−8421.
(85) Lilien, R. H., Stevens, B. W., Anderson, A. C., and Donald, B. R. (2005) A novel ensemble-based scoring and search algorithm for protein redesign and its application to modify the substrate specificity of the gramicidin synthetase a phenylalanine adenylation enzyme. *J. Comput. Biol. 12*, 740−761.
(86) Lidl, R., and Neiderreiter, H. (1983) Finite fields. In *Encyclopedia of Mathematics and its Applications*, Addision-Wesley, Reading, MA.
(87) Miller, B. R., III, McGee, T. D., Jr, Swails, J. M., Homeyer, N., Gohlke, H., and Roitberg, A. E. (2012) MMPBSA. py: An efficient program for end-state free energy calculations. *J. Chem. Theory Comput. 8*, 3314−3321.
(88) Katragadda, M., Magotti, P., Sfyroera, G., and Lambris, J. D. (2006) Hydrophobic effect and hydrogen bonds account for the improved activity of a complement inhibitor, compstatin. *J. Med. Chem. 49*, 4616−4622.